

Blends of Poly(methacrylate) Block Copolymers with Photoaddressable Segments

Thomas Breiner,[†] Klaus Kreger,[†] Rainer Hagen,[‡] Michael Häckel,[§] Lothar Kador,[§] Axel H. E. Müller,[‡] Edward J. Kramer,^{||} and Hans-Werner Schmidt*

Makromolekulare Chemie I, Makromolekulare Chemie II, and Experimentalphysik and Bayreuther Institut für Makromolekülforschung, Universität Bayreuth, D-95440 Bayreuth, Germany, Zentrale Forschung/Informationstechnologie, Bayer AG, 51368 Leverkusen, Germany and Materials Department, University of California at Santa Barbara, Santa Barbara, California, 93106

Received October 27, 2006; Revised Manuscript Received December 6, 2006

ABSTRACT: The paper presents the synthesis of azobenzene-functionalized block copolymers based on a poly(methyl methacrylate) (PMMA) segment and an azobenzene-functionalized poly(hydroxyethyl methacrylate) segment, and a basic study of blending these block copolymers with homopolymers is given. Two diblock copolymers, prepared via different routes, were synthesized by a living anionic polymerization followed by a polymer analogous reaction to attach the azobenzene side groups. Self-assembly of the block copolymers resulted in phase-separated morphologies on the nanometer scale. The photoaddressable azobenzene segments are dispersed in the PMMA matrix and locally confined. Special focus is given to the preparation and characterization of block copolymer blends with PMMA homopolymer in order to dilute the phase-separated azobenzene morphology and reduce the optical density while maintaining the confinement. The block copolymer blends were characterized with respect to their morphology and initial holographic experiments were performed.

1. Introduction

In the past few decades, the amount of information to be stored has rapidly increased and will increase even more strongly in the future. This development has led to an intensive search for new materials for optical data storage technologies. Optical data storage is commercially established and the storage capacity and data transfer rates dramatically increased from CD-ROM to multilayer DVD products. However the future demand on storage capacity and transfer rates is limited with the concept of two-dimensional storage and stacking several layers. A promising solution, besides near field recording, is the holography by employing the third dimension and in such utilizing the entire volume. The concept, fundamental issues underlying holographic data storage and the current status in the materials development have been reviewed recently by Hesselink et al.¹ and Ashley et al.² The most promising organic-based materials under consideration for this application include photopolymer systems based on an optimized photopolymer^{3,4} and photosensitive media composed of two independently polymerizable and compatible monomers.⁵ In contrast to these systems, which can only be written once, a rewritable class of materials consists of photoaddressable polymers (PAP) containing azobenzene moieties. Polymers with photoaddressable azobenzene side chains were first introduced by Ringsdorf et al.^{6,7} Their applicability to holographic data storage was described by various groups.^{8–10} Over the years, many different polymer systems were synthesized and the photoinduced trans–cis–trans isomerization of the azobenzene chromophores was investigated also in view of an application in optical data storage. For instance, Hvilsted et

al. reported the synthesis and characterization of various polyesters with liquid-crystalline azobenzene side groups¹¹ and also of peptide oligomers containing similar chromophores.¹² Random methacrylate copolymers with azobenzene side groups were studied by Zilker et al.^{13,14} and Hagen and Bieringer.¹⁵

One challenge for data storage applications is that homopolymers as well as copolymers containing azo-moieties tend to develop surface relief gratings in addition to the desired bulk refractive-index modulation when exposed to a light intensity grating.^{16–18} Being thin gratings, the surface reliefs are detrimental to angle-multiplexed inscriptions with high angular sensitivity. A number of mechanisms were proposed to explain the massive transport of the material, which occurs even at low light intensities.^{19–22} A solution to this issue was found utilizing block copolymers, in which the chromophores are confined in the minority phase so that macroscopic material transport is precluded.²³ In addition, to superimpose several holographic gratings at the same spot, thick samples are required. Block copolymers with azobenzene-containing side chains were also synthesized by various other groups.^{24–39} However, less data were given concerning holographic experiments utilizing thick films, in particular regarding angular multiplexing. In thick films, the optical density of the entire sample has to be sufficiently low. One possibility to reduce the optical density is a random copolymer with nonabsorbing comonomers. However, this approach faces the problem that the cooperative effect of the azobenzene side groups is lost and the stability of holographic gratings is limited. In our previous work, we demonstrated that block copolymers based on polystyrene segments and azobenzene-functionalized polybutadiene segments are, due to the nanophase separation, suitable in terms of writing and stability of inscribed holographic information.^{23,40,41} However for angular multiplexing, thicker samples with an optical density in the range of 0.7 are required. Minabe et al. achieved this by blending an azo-containing homopolymer with a nonabsorbing polymer.⁴² It is also possible to blend the above-mentioned polystyrene-

* Corresponding author. Telephone/fax: +49-921-553200/553206. E-mail address: hans-werner.schmidt@uni-bayreuth.de.

[†] Makromolekulare Chemie I, Universität Bayreuth.

[‡] Makromolekulare Chemie II, Universität Bayreuth.

[§] Experimentalphysik and Bayreuther Institut für Makromolekülforschung, Universität Bayreuth.

[‡] Zentrale Forschung/Informationstechnologie, Bayer AG.

^{||} Materials Department, University of California at Santa Barbara.

block-azobenzene-functionalized polybutadiene blockcopolymers with polystyrene homopolymer in order to achieve thick samples for angular multiplexing.^{41,43}

In this paper, we present the synthesis and characterization of block copolymers consisting of a PMMA block and a poly-(2-hydroxyethyl methacrylate) (PHEMA) block substituted with azobenzene chromophore side groups. This concept utilizes the self-assembly of block copolymers into a microphase-separated structure to reduce optical density while maintaining the cooperative effect and allowing the fabrication of millimeter-thick samples with feasible optical density and high optical quality. Both segments of the block copolymer, the one forming the inert matrix as well as the photoaddressable one, are based on a methacrylate backbone which assures good optical quality. Furthermore, this system allows us to investigate the morphology of the phase-separated block copolymers as well as the blended block copolymers by common methods in a proper way. This in turn verifies the results, which we obtained by holographic grating experiments with similar polymers.^{40,43,44} In the following, these azobenzene-functionalized block copolymers will be called PABCP as an abbreviation for **photoaddressable block copolymers**.

2. Experimental Part

2.1. Synthesis of Photoaddressable Block Copolymers. Block copolymers composed of one segment with repeating units functionalized with an azobenzene side group and an inert PMMA block were obtained via a two-step synthesis. Two different approaches were chosen to yield two block copolymers that vary in their total molecular weight but provide a comparable ratio of the two segments. For both block copolymers, the two segments (PMMA and silyl-protected PHEMA) were synthesized by sequential anionic polymerization. After deprotection to the hydroxy group, the azobenzene side group was attached via a polymer analogous reaction.

If not otherwise noted, chemicals were obtained from Aldrich and used without further purification. Tetrahydrofuran (THF) as solvent for the polymerization and polymer analogous reaction was first refluxed and distilled over calcium hydride (CaH₂) and freshly distilled from potassium before usage. LiCl was dried under high vacuum at 250 °C for several days before being dissolved in THF. 1,1-diphenyl-3-methylpentyllithium (DPHLi) as initiator for the anionic polymerization was generated *in situ* by the reaction of *sec*-butyllithium (1.3M solution in hexane) with an excess of 1,1-diphenylethylene in THF at -60 °C. MMA was purified as described in the literature.⁴⁵ Triethylamine for the esterification reaction was refluxed over CaH₂ and then distilled.

Poly(methyl methacrylate)-*b*-poly(2-hydroxy-ethylmethacrylate) (PMMA-*b*-PHEMA), 1c. Trimethylsilyloxyethyl methacrylate (TMS-OEMA) was purified according to a procedure described by Nakahama et al.^{46, 47} The block copolymer was obtained by anionic polymerization of MMA in THF at -78 °C with LiCl as additive. A sample of the precursor polymer was terminated with degassed methanol yielding **1a**. Subsequently TMS-OEMA was added to the solution. Finally, the living chain ends were terminated by adding degassed methanol. The trimethylsilyl- (TMS-) protecting group is cleaved during the precipitation of the reaction mixture in methanol as indicated by the absence of the signal at 0.1 ppm in the ¹H NMR spectrum. Therefore, **1b** cannot be isolated.

Poly(2-hydroxyethylmethacrylate)-*b*-poly(methyl methacrylate) (PHEMA-*b*-PMMA), 2c. The synthesis of the second block copolymer was carried out slightly differently from the one described above. *tert*-Butyldimethylsilyl was chosen as the protecting group for the HEMA due to a change in the sequence of monomer addition. Synthesis and reaction conditions for the anionic polymerization of *tert*-butyldimethylsilyloxyethyl methacrylate (TBDMS-HEMA) were similar to those reported in the literature.^{47,48} First TBDMS-HEMA was polymerized at -60 °C in THF with

LiCl for 60 min. The temperature was lowered to -78 °C and MMA as second monomer was added. The living chain ends were terminated by adding degassed methanol. Universal calibration and the Mark-Houwink parameters of P(TBDMS)⁴⁸ were used to obtain the absolute molecular weight of the first block (P(TBDMS-HEMA)). The ratio between the PMMA and the silyl protected PHEMA segments of **2b** was determined by ¹H NMR spectroscopy. The cleavage of the protecting group was performed in dioxane using diluted hydrochloric acid as catalyst yielding **2c**.

Polymer Analogous Reaction with Block Copolymers. In a typical procedure, an excess of an acid chloride and the hydroxy-substituted block copolymer were dissolved in anhydrous THF. A large excess of triethylamine compared to the acid chloride was added to the solution of the block copolymer before both reactants were combined and refluxed for 3 days. Upon completion of the reaction, excess ethanol was added to convert the excess of the acid chloride into the more soluble ester compound. Pure functionalized block copolymer was obtained by several cycles of dissolution and precipitation of the polymer. Polymer analogous reaction of **1c** with benzoyl chloride yields **1e**. The composition between the PMMA and the PHEMA segments of **1c** was determined by ¹H NMR spectroscopy of **1e**. Table 1 summarizes the characteristic physical data for the two azobenzene-functionalized block copolymers **1d** and **2d**.

Poly(2-(4-(phenylazo)benzoate)ethyl methacrylate) (3). Trimethylsilyloxyethyl methacrylate (TMS-OEMA) was purified according to a procedure described by Nakahama et al.^{46,47} The PHEMA was obtained by anionic polymerization in the same way as mentioned above. The living chain ends were terminated by adding degassed methanol. The trimethylsilyl- (TMS-) protecting group is cleaved during the precipitation of the reaction mixture in methanol. The poly(2-(4-(phenylazo)benzoate)ethyl methacrylate) (**3**) was obtained by a polymer analogous reaction with 4-(phenylazo)benzoyl chloride in the same way as mentioned above.

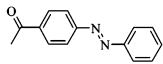
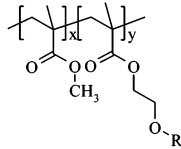
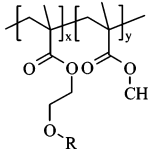
PMMA (4). The PMMA homopolymer for the binary blends was synthesized by anionic polymerization in the same way as mentioned above.

2.2. Film Preparation. Samples for holographic grating experiments were prepared by casting a filtered 5 wt % THF solution in a glass container with a flat bottom. The solutions were slowly evaporated over a period of one week to allow the formation of the morphology close to the thermodynamic equilibrium. The as-cast polymer films were dried under vacuum for two days at room temperature, followed by annealing for 8 h at 160 °C. Finally, the samples were placed between two glass plates, shortly heated to 200 °C and slightly pressed to obtain films with a thickness in the range of some tens of micrometers. This method results in a good adhesion between sample and glass substrate. All samples showed good optical properties and absence of undesired scattering.

2.3. Characterization. Morphology studies of the azobenzene-functionalized block copolymers and blends were performed on a Zeiss 902 transmission electron microscope operating at 80 kV. Ultrathin sections were obtained using a Reichert ultramicrotome equipped with a diamond knife. The specimens were stained using ruthenium tetroxide vapor. In order to exclude any change in the morphology during sample preparation, the specimens were cut from the same samples on which the holographic grating experiments were performed.

X-ray transmission measurements were performed at the Cornell High-Energy Synchrotron Source (CHESS). The beamline at CHESS employs a 2D charge coupled detector (CCD) (1024 × 1024 pixels at 51 μm/pixel resolution) and the sample-to-detector distance was set at 984 mm with a wavelength of 0.155 nm. The specimens for dynamic secondary ion mass spectroscopy (SIMS) were prepared by spin coating a 2.5% toluene solution onto a silicon wafer covered by a 200 Å silicon nitride layer. The concentration of the polymer solution and the rotational speed of the sample were adjusted to obtain films of about 380 nm. Subsequently, the films were annealed in a high vacuum oven at 180 °C for 24 h. SIMS was performed on a Physical Electronics 6650 quadrupole instrument. Using a 30 nA, 3 kV O₂⁺ primary beam, 30 μm in diameter,

Table 1. Structure and Molecular Weight Characterization of the Synthesized Azobenzene-functionalized Diblock Copolymers

Polymer	Structure		M_n^a (absolute) [g/mol]	Segment		PDI ^c
	R=					
1d			42400	PMMA (y) [g/mol], (DP ^b)	P(Azo-EMA) (x) [g/mol], (DP ^b)	1.11
				32000 (320)	10400 (31)	
2d			152900	P(Azo-EMA) (x) [g/mol], (DP ^b)	PMMA (y) [g/mol], (DP ^b)	1.09
				35900 (106)	116700 (1167)	

^a Calculated from the absolute molecular weight of the precursor obtained by GPC in combination with the ¹H NMR data of the block copolymer ^b Degree of polymerization (DP) ^c Polydispersity index (PDI)

scanned over a 300 × 300 μm area, negatively charged secondary ions were collected from the central 15% of the crater area. A static, defocused 400 V electron beam was used for charge compensation. ¹H NMR data were obtained from a Bruker AC 250.0 (250 MHz) spectrometer using *d*-chloroform as solvent. Molecular weights were obtained by GPC using THF as eluent (columns: PSS SDV–Gel (5 μm), 10⁵, 10⁴, 10³, 100 Å).

2.4. Setup for Holographic Grating Experiment. A setup similar to the one described by other groups was used to carry out the holographic grating experiment.^{14,49} All experiments were performed at ambient conditions. Two s-polarized beams (wavelength 532 nm, *I* = 100 mW/cm²) of a tunable krypton laser with a beam size of about 3 mm in diameter were intersected in the polymer sample. The incidence of the writing beams occurs symmetrical and perpendicular to the sample with an angle between the writing beams (2Θ = 10°). Simultaneously, a HeNe laser (wavelength 633 nm) was used to probe the holographic grating. The spot size was chosen to be less than 1 mm in diameter with an intensity of about 15 mW/cm². Photodiodes were used to determine the diffracted and the transmitted writing beams in order to obtain the diffraction efficiency, *η*, as a function of time. The film thickness (*d*) of the studied blends varied in a range of 68 to 90 μm. The refractive index modulation, Δ*n*, was calculated according to Kogelnik's theory,⁵⁰ which describes the diffraction of light on thick absorption and diffraction gratings against the angle as well as the wavelength of the incident light. In the case of small refractive index modulations one can assume the following equation:

$$\eta \approx \left(\frac{\pi d \Delta n}{\lambda_{\text{read}} \cos \Theta} \right)^2$$

3. Results and Discussion

3.1. Synthesis and Characterization of Azobenzene-Functionalized Block Copolymers. Anionic polymerization of MMA and silyl-protected HEMA was carried out to prepare well-defined starting block copolymers for further polymer analogous reactions. This approach avoids limitations in the degree of polymerization and molecular weight distribution due to side reactions which have been usually observed in the direct anionic polymerization of azo-functionalized monomers.^{51,52} Usage of PHEMA provides some advantages compared to concepts in which the hydroxyl group is obtained by hydroboration reaction of pendent double bonds in poly(1,2-dienes)^{25,53,54} such as shorter reaction times compared to isoprene or lower

toxicity than butadiene. Furthermore, the remaining double bonds in the backbone of the polydiene decrease the thermal stability of the functionalized block copolymer. As shown in Figure 1, we employed two routes with different silyl-protecting groups in the polymerization of the HEMA monomer to obtain the diblock copolymers.

In the first case, commercially available 2-[(trimethylsilyl)-oxy]ethyl methacrylate (TMS–OEMA) was added at a temperature of −78 °C to the living chain of the PMMA block. While the chosen reaction conditions allow a controlled polymerization of both monomers,^{46,47,55} a major drawback of this polymerization sequence results from possible termination. Because of the chosen composition, the formed homopolymer is difficult to detect and remove from the block copolymer. This is due to the solubility behavior of PMMA-*b*-PHEMA which is mainly determined by the molecular weight of the PMMA precursor (32 kg/mol) and not by the PHEMA (4 kg/mol) segment. As seen from the GPC traces in Figure 2, the apparent molecular weight of the PHEMA containing diblock copolymer **1c** decreases slightly to that of the isolated PMMA precursor **1a** (A-block).

The intramolecular H-bonding leads to a decrease in the radius of gyration and therefore a smaller hydrodynamic volume for the block copolymer **1c** compared to a PMMA block **1a**.⁵⁶ The slightly higher polydispersity of the hydroxy functionalized diblock (PDI = 1.11) compared to the PMMA precursor (1.08) and the benzoylated diblock copolymer of **1c** (**1e**) might be caused by an unfavorable interaction of the THF less soluble PHEMA block with the GPC column material (Figure 2). Absolute molecular weights were determined by GPC result of the precursor using a PMMA calibration in combination with the ¹H NMR data of the benzoylated block copolymer.

For the synthesis of the block copolymer **2c**, the sequence of monomer addition during the anionic polymerization was reversed. In addition, 2-[(*tert*-butyldimethylsilyl)oxy]ethyl methacrylate (TBDMS–OEMA) that uses the more stable *tert*-butyldimethylsilyl (TBDMS) protecting group was chosen as HEMA derivative. No side reactions of the anionic chain end of the PMMA with the silyl group or ester linkage in the (TBDMS–OEMA) repeating unit were observed during the MMA polymerization. The enhanced stability of this silyl-

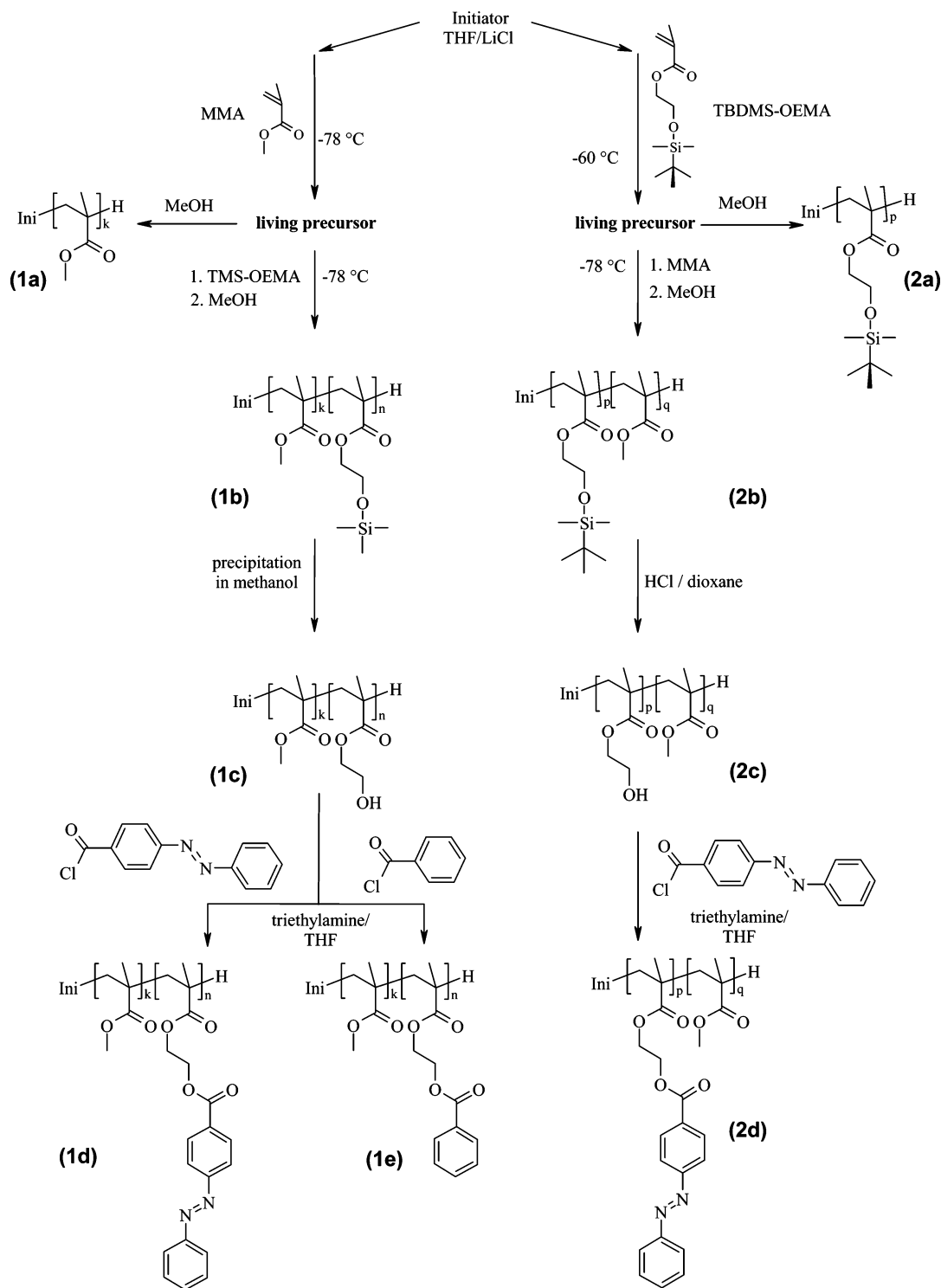


Figure 1. Synthesis of azo-functionalized block copolymers **1d** and **2d**, including the reference polymer **1e** for analytical purpose.

protected HEMA in anionic polymerization was reported earlier by Nakahama et al.⁴⁷ and has been studied recently in detail at our laboratory.⁴⁸ The change of the polymerization sequence of the protected HEMA and MMA monomers facilitates the extraction of a possible termination product that is formed during addition of the second monomer. The short homopolymer of PHEMA can be removed easily by precipitation of the deprotected polymer from dioxane into methanol due to the large difference in solubility compared with **2c**, which possesses a large less polar PMMA segment. Pan et al. used a similar strategy for the anionic synthesis of their PHEMA-*b*-PMMA diblock copolymers.⁵⁷ Their molecular weight of the block

copolymer (4200 g/mol) and the PHEMA (400 g/mol), however, was small compared to our PHEMA segment, which possesses an average degree of polymerization of about 106 repeating units corresponding to a molecular weight of about 13.8 kg/mol. As seen from the comparison of the block copolymers **1c** and **2c**, the stoichiometry in the polymerizations was adjusted to result in similar ratio of A to B repeating units for **1c** and **2c** but significantly different total molecular weights. The ratio of MMA to HEMA repeating units was determined by ¹H NMR for **1c** as 11.0 and for **2c** as 10.3.

Both diblock copolymers **1c** and **2c** were functionalized by an esterification reaction of the PHEMA segment with an excess

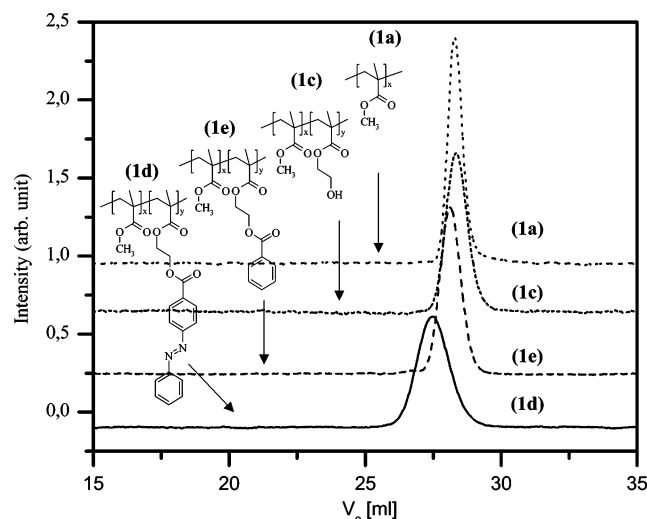


Figure 2. RI signal GPC traces of block copolymers and the corresponding precursor polymer: **(1a)** isolated PMMA A-block (...); **(1c)** PMMA-*b*-PHEMA (---); **(1d)** PMMA-*b*-poly(2-(4-(phenylazo)-benzoate)ethyl methacrylate) (-.-); **(1e)** PMMA-*b*-poly(2-benzoyloxyethyl methacrylate) (—).

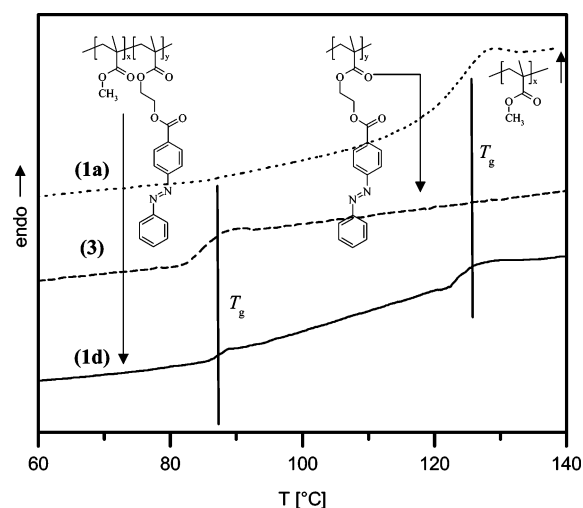


Figure 3. DSC second heating curves at a rate of 10 °C/min of **(1a)** isolated PMMA A-block (...), **(1d)** PMMA-*b*-poly(2-(4-(phenylazo)-benzoate)ethyl methacrylate) (-.-), and **(3)** Poly(2-(4-(phenylazo)-benzoate)ethyl methacrylate) (—).

(1.5 fold) of 4-(phenylazo)benzoyl chloride (Figure 1). Virtually complete conversion was achieved by carrying out the reaction at elevated temperature (60 °C) in combination with triethylamine as base. The conversion of the hydroxy into an ester group was checked by IR spectroscopy probing the change of the signal at 3430 cm⁻¹. After extraction, absence of the excess amount of azo chromophore greater than 0.2 wt % referred to the attached chromophore was demonstrated by integration of the UV trace at 340 nm in the GPC elugram. A slight broadening of the molecular weight distribution for **1d** (PDI = 1.11) (Figure 2) and for **2d** (PDI = 1.09) was observed after the polymer analogous reaction. As expected, both azobenzene-functionalized block copolymers revealed a higher apparent molecular weight in the GPC elugram compared to the one of the benzylated and hydroxy-functionalized diblock copolymers (Figure 2).

Azobenzene substituted block copolymers **1d** and **2d** each show two independent glass transitions corresponding to the azobenzene-functionalized PHEMA segment (87 °C) and the PMMA matrix (126 °C). Figure 3 presents the DSC traces for the block copolymer **1d** in comparison to the corresponding homopolymers **1a** and **3**.

Both T_g s found for the azo-functionalized block copolymer agree well with the transitions of the individual homopolymers, suggesting the formation of a microphase-separated structure with a small interface between both blocks. As shown in Figure 4, transmission electron micrographs of the THF cast films also reveal a microphase-separated structure for both azo-functionalized block copolymers.

Because of selective staining with ruthenium tetroxide (RuO₄), the dark areas correspond to the azobenzene-functionalized block while the unstained PMMA matrix remains bright. For the higher molecular weight block copolymer **2d**, a cylindrical morphology is recognized in the micrograph in Figure 4b. The dark round areas correspond to cross sections of cylinders cut perpendicularly to their main axis; the lamellar-like structure is related to a cut parallel to the main axis. In contrast, TEM of **1d** (Figure 4a) only reveals phase separation while the exact type is difficult to determine. In some regions, cylinders cut perpendicularly and along their axes can be seen but long-range order is missing. As expected, a comparison of the cylinders in the micrographs **4a** and **4b** shows that their diameter scales with the block length of the minority part as well as with the molecular weight of the corresponding block copolymers **1d** and **2d**, respectively. For block copolymer **1d**, a diameter of about 12 ± 1.5 nm for the cylinder was estimated from TEM and about 17 ± 3 nm for **2d**. The blurring in the micrograph results from the partial degradation of the PMMA matrix due to radiation damage from the electron beam.^{58,59} Therefore, an accurate value for the average cylindrical long period is not obtained from TEM.

3.2. Preparation and Characterization of Binary Blends with Azobenzene-Functionalized Diblock Copolymers. Binary blends from both PABCP (**1d** and **2d**) and anionically synthesized PMMA (**4**) with a molecular weight of 40 kg/mol and a PDI of 1.05 were prepared as described in the experimental part 2.2. The molecular weight of the homopolymer **4** was chosen to be similar (**1d**) or smaller (**2d**) than that of the PMMA segment of the block copolymers. The weight fraction of the PMMA homopolymer **4** was adjusted to yield a total PMMA weight fraction of 0.87 to 0.96 (Table 2).

The good optical properties of all blends indicate the absence of macrophase separation. TEM and X-ray scattering was used to investigate the morphology of the specimen. The transmission electron micrograph of blend **B** consisting of 36 wt % of block copolymer **1d** and 64 wt % of PMMA homopolymer **4** is shown in Figure 5.

Because of the staining conditions with RuO₄, the azobenzene-functionalized segments appear as dark spheres randomly distributed within the unstained PMMA matrix. As expected, the higher molecular weight of the azobenzene-functionalized segment in blends **2d** leads to a larger average radius of the spheres (8.0 ± 0.8 nm) compared to that derived from blends of block copolymer **1d** (6.0 ± 0.7 nm). In all images of this series, the volume fraction of the spheres appears to be much higher than expected from the composition of the blends summarized in Table 2. Two explanations can be given for this observation: First, more than one layer of spheres might be imaged because of the specimen's thickness. Furthermore, radiation damage of PMMA by the electron beam has been described in the literature^{58,59} and no information is available regarding stability of the azobenzene-functionalized PHEMA. However, a much higher stability of the chromophore-containing segment compared to PMMA is expected due to a stabilizing effect of the aromatic character of the azobenzene side groups. Their stabilizing effect on the environment over a range of more

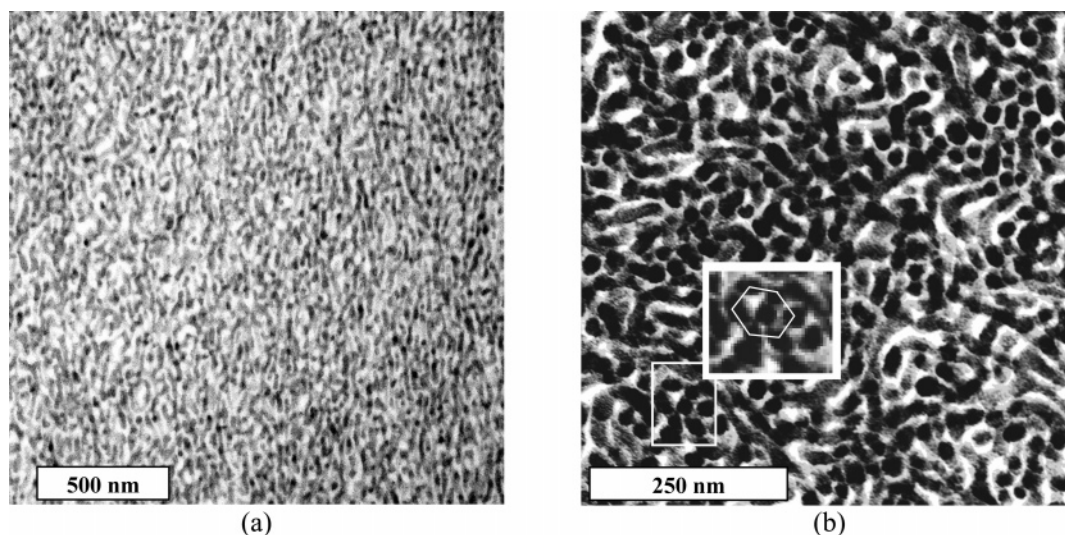


Figure 4. Transmission electron micrographs of block copolymers **1d** (a) and **2d** (b) Staining of the azo-dye containing phase with ruthenium tetroxide (dark phase).

Table 2. Overview of the PABCP Blends from Azobenzene-Functionalized Diblock Copolymers and the PMMA Homopolymer

blend	block copolymer	weight fraction $\times 100$			radius of spheres [nm] ^a
		block copolymer	homopolymer PMMA (4)	total PMMA	
A	1d	50	50	88.5	5.8 ± 0.6
B	1d	36	64	91.8	5.9 ± 0.7
C	1d	16	84	96.4	5.8 ± 0.7
D	2d	50	50	87.7	8.1 ± 0.8
E	2d	29	71	93	8.0 ± 0.8
F	2d	20	80	95	8.0 ± 0.9

^a Determined by TEM.

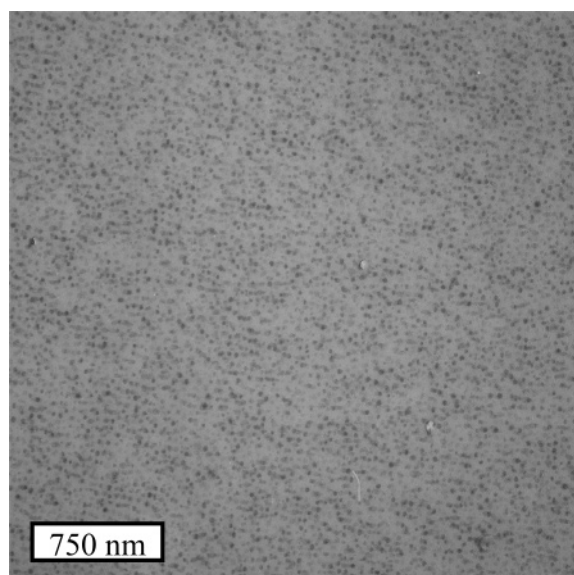


Figure 5. Transmission electron micrographs of the PABCP blend **B** (36 wt % block copolymer **1c**, 64 wt % homopolymer **4**) Staining of the azo-dye containing phase with rutheniumtetroxide (dark phase).

than one nanometer reduces the sensitivity of other chemical groups toward radiation damage.⁶⁰ For this reason, we used a combination of secondary ion mass spectroscopy (SIMS) and atomic force microscopy (AFM) in the two selected blends **D** and **E** to examine the accuracy of the feature size obtained from TEM. Films in the thickness range of 400 nm are partially etched by SIMS and the exposed surface is subsequently studied by AFM. This approach is similar to the one introduced by

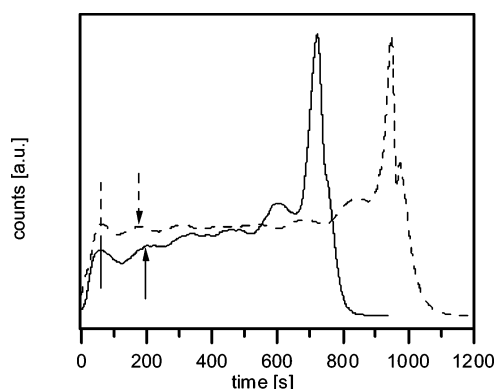


Figure 6. Secondary ion mass spectroscopy depth profile for blend **D** (---) with a thickness of ca. 500 nm and **E** (—) with a thickness of ca. 350 nm. Shown is the signal for the CN fragments. The specimens were spin coated from toluene, annealed 18 h at 180 °C (CN signal derives from the azobenzene group).

Yokoyama et al. who studied the structure of asymmetric polystyrene-*b*-poly(2-vinylpyridine) diblock copolymers in thin films.⁶¹ In the PABCP blends presented here, the CN fragments of the azobenzene group lead to a distinguishable signal compared to the PMMA matrix. For a layer structure of spheres, a sinusoidal intensity profile of the CN signal is expected. The carbon signal originating from both blocks remains constant during the etching process until the substrate is reached. Figure 6 presents the CN signal for the two blends **D** and **E**.

As expected from the increasing volume fraction of PMMA for **E** compared to **D**, the distance between the maximum CN signal increases in the SIMS depth profile. High degree of order is observed only near the surface and the interface off/to the silicon wafer. The intense peaks for the CN signal at 700 and 950 s originate from charging problems and can be considered as an artifact. In order to study the size of the spheres by AFM for each of the two samples, the etching process was stopped as the second maximum of the CN signal was reached (arrow in Figure 6). Reaching the highest possible number of spheres etched midway, a maximum in the cross section of spheres is reached and hence a maximum in the generation of CN fragments is detected. The exposed surface was imaged by AFM in this manner. Figure 7 presents the height image of the surface in the crater of blend **D**.

As the azobenzene-functionalized PHEMA possesses a higher etching rate compared to PMMA, it appears in the height image

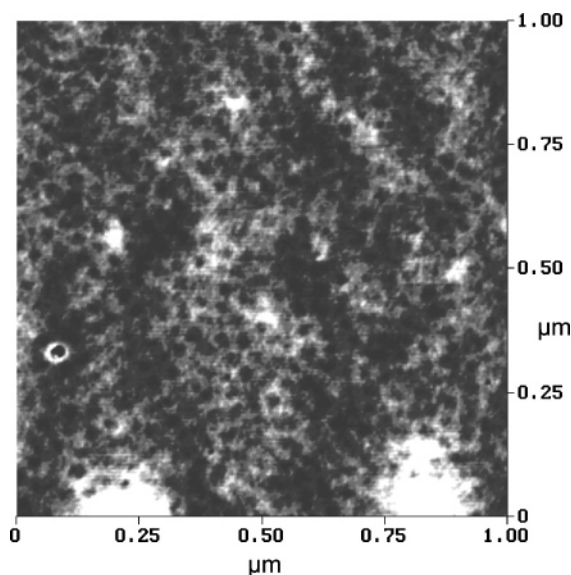


Figure 7. Atomic force micrograph taken from blend **D** after etching the surface with O_2^+ in the Secondary Ion Mass Spectroscopy, Specimen spin coated from toluene, annealed 18 h at 180 °C, thickness ~ 350 nm.

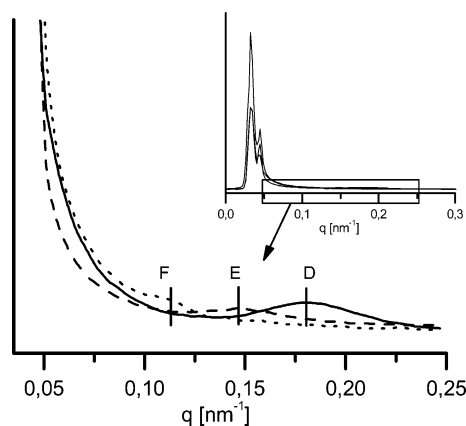


Figure 8. Small-angle X-ray diffraction pattern of the blends **D**, **E**, and **F** based on block copolymer **2d** and PMMA homopolymer **4**: **D** (total PMMA amount 87.7 wt %) (—); **E** (total PMMA amount 93 wt %) (---); **F** (total PMMA amount 95 wt %) (····).

as holes (dark spots) within the matrix. In both blends, an average diameter of 14 ± 2 nm was found for the spheres. As both studied blends show a comparable size of the spheres, we conclude that the added PMMA homopolymer sequesters homogeneously into the PMMA matrix. It does not lead to a swelling of the photoaddressable azobenzene containing phase. As a result, the size of the spheres remains constant while the distance between them increases. Furthermore, the data are consistent with those obtained from TEM for the dimensions of the spheres (16 ± 1.6 nm). This result suggests that it is indeed valid to use TEM to verify the absence of swelling of the photoaddressable segment and to determine the average size of the spheres. These results suggest also that the distance between the spheres increases proportionately with the fraction of added PMMA homopolymer; small-angle X-ray scattering is used to verify this assumption. Figure 8 presents the diffraction pattern of the three blends, **D**, **E**, and **F**.

Because of the lack of long-range order, only one broad reflex is observed for all three blends. It corresponds to an average correlation length and allows the calculation of an average distance between the spheres. The average distance increases from 34.8 (**D**) to 43.3 (**E**) and 54.5 nm (**F**) with an increase in

the total PMMA weight fraction from 0.877 to 0.95. This observation is consistent with theoretical predictions of phase separation in primary blends.^{62–64} For blends from block copolymer **2d**, the molecular weight of PMMA homopolymer is much smaller compared to the PMMA segment of the block copolymer and expands selectively in the matrix. Very similar results were obtained for all blends prepared from block copolymer **1d**, which shows a spherical morphology although molecular weight of the PMMA homopolymer is comparable to that of the PMMA segment of the block copolymer.

3.3. Holographic Grating Experiments in Binary Blends from Azobenzene-Functionalized Diblock Copolymers. The influence of photoaddressable segments localized in domains of nanometer size on the refractive index was studied by holographic grating experiments. From the grating experiment, the diffraction efficiency, η , is obtained. The refractive index modulation, Δn , was calculated according to Kogelniks theory.⁵⁰ In order to compare the different series of the blends, Δn was corrected by the weight fraction of the azo chromophore content in the blend. The advantage of the parameter Δn_{norm} consists of its independency from the fraction of azo-chromophore.

In Figure 9, Δn_{norm} for both series of blends is plotted as a function of illumination and relaxation time.

The laser was turned on at time zero and a holographic lattice was written while η was measured using a reading wavelength of 633 nm. This wavelength ensures that no trans–cis excitation occurs during the reading process. After 3600 s, the writing beams were turned off and the decay of Δn was monitored for a further 1800 s. In both series of blends, the increase and the decay of Δn follow similar kinetics independent of the concentration of chromophore in the sample.

Within each set of blends, the growing and the relaxation curves show a very similar behavior independent of the amount of added homopolymer. The difference in the data within the two sets of blends **A–C** and **D–F** is within the error margin. We can conclude that the spatial distance between the spheres has no influence on the kinetics of Δn_{norm} and its maximum achievable value. This result was already expected from the microstructure of the samples which revealed the same size of the photoaddressable domain for each specimen in one set of blends. A comparison of samples from the two sets of blends reveals slight differences including the growing curve as well as the maximum achievable Δn_{norm} . In the first 100 s, all specimens behave virtually identically independent of the amount of added homopolymer or the molecular weight of the block copolymer and hence the domain size of the photoaddressable domain. This behavior indicates that the first stage in both series of blends follows a similar kinetic for the orientation of the azo chromophores. Subsequently, differences in their holographic growing curve appear: The Δn_{norm} of the specimens **D–F** shows a slightly higher rise compared to the blends **A–C**.

The time dependency of the birefringence during the holographic writing process seems to be a result of two different response modes in terms of orientation of the azo chromophores perpendicular to the polarization of the laser beam. We believe that this result reflects the dynamics of azobenzene groups in various environments. It was shown earlier that the orientation and relaxation process depends on the environment of the azo chromophores as shown in samples with a rigid or viscoelastic surrounding matrix.^{65,66} The blends in the current work undergo phase separation into a spherical morphology in which the photoaddressable segment is dispersed in a rigid matrix of PMMA. The T_g of both domains, the surrounding continuous matrix (126 °C) and the photoaddressable spheres (87 °C),

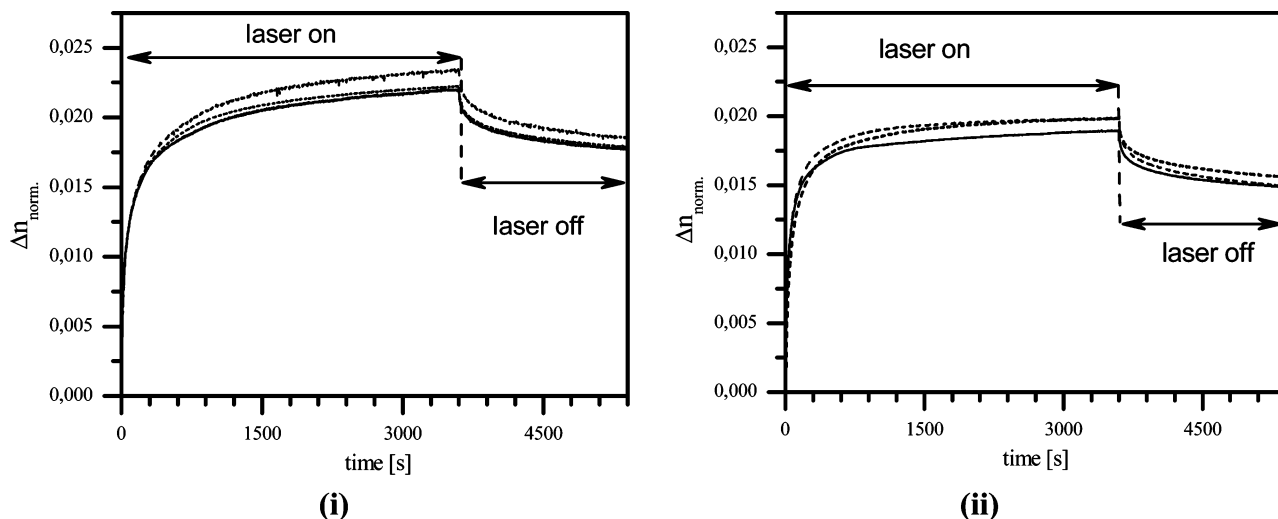


Figure 9. Growing (laser on) and decay (laser off) of the normalized induced birefringence ($\Delta n_{\text{norm.}}$) of polymeric films vs time. $\Delta n_{\text{norm.}}$ is normalized with respect to the azo content (Writing time: 3600 s, writing wavelength: 532 nm, Intensity: 100 mW/cm², reading wavelength: 633 nm). Left (i): samples of blends **A** (—), **B** (---), and **C** (····) consisting of the azofunctionalized blockcopolymer **1b** and the PMMA homopolymer **4**. Right (ii): samples of blends **D** (—), **E** (---), and **F** (····) based on the azofunctionalized blockcopolymer **2b** and the PMMA homopolymer **4**.

corresponds to that of the homopolymers equivalent to a difference of almost 40 °C. Hence, azo chromophores encounter different environments depending whether they are located in the outer shell of the sphere close to the interface to the PMMA matrix or closer to the center of the sphere. We assume that these chromophores show an orientation behavior comparable to the one in an azobenzene-functionalized homopolymer. For the azobenzene chromophores in the outer shell of the spheres, an influence from the surrounding matrix may be possible. The volume of a sphere scales with the radius to the third order compared to the second order of the surface area. Consequently, a given volume distributed on several smaller spheres compared to fewer large ones results in an increase of surface area. The molecular weight of the azo-chromophore functionalized segment differs between the blends **A–C** and **D–F** by a factor of about 4, resulting in a difference in the surface area of about a factor of 2 assuming that the radius of gyration is proportional to the square root of the molecular weight for both PABCP. The azo chromophores located near the interface to the PMMA experience less unfavorable dipolar interactions from neighboring azobenzene side groups and hence show a higher inducible $\Delta n_{\text{norm.}}$. For this reason, the maximum inducible Δn of the blends **A–C** exceeds that of the blends **D–F**, but the time frame to reach the maximum Δn significantly increases for the smaller spheres. A comparison of both series of blends shows that the azo chromophores in the smaller spheres undergo a stronger relaxation resulting in a loss of about 32% of induced birefringence compared to the blends **D–F** (~20%) of the larger spheres. Two different processes contribute to the decay of induced birefringence. The main portion of relaxation occurs in the first few seconds after the beam is turned off (25%) and shows a characteristic similar to the one reported for various amorphous azo-chromophore functionalized PAPs.^{67,68} The fast decay mainly results from motions arising from heat dissipation.^{68,69}

Conclusion

We have presented a new material concept for photoaddressable polymers with which the fraction of azo chromophore can be widely reduced and samples with millimeter thickness and low optical density can be prepared. Such materials could be used for holographic multiplexing in thick films. Two different

block copolymers with a PHEMA and a PMMA segment were synthesized in which PMMA forms the matrix. In both block copolymers, the ratio of the two blocks remains nearly constant while the molecular weight of the segments is altered. The attachment of a structural simple azobenzene side group results in phase-separated block copolymers. Addition of PMMA homopolymer leads to the formation of a spherical morphology in which the photoaddressable domain is dispersed in an inert matrix of PMMA. We prepared a set of blends for each of the two azobenzene-functionalized block copolymers. Within each set of blends, the weight fraction of the photoaddressable segment was systematically altered in the range of 3.6–11.5 wt % and 5–12.3 wt %. All blends possessed a spherical morphology as verified by TEM. Furthermore, we have shown that PMMA homopolymer solubilizes preferentially in the PMMA matrix and swelling of the spheres does not occur in the blends. Initial holographic experiments were performed. From the refractive index modulation of the different blends, one sees that they are independent from the homopolymer amount. This is in agreement with the results of the morphology characterization methods.

Acknowledgment. The authors thank Tom Mates (UCSB) for SIMS and Astrid Gödel for TEM. Dr. Marco Huber and Dr. Stephan Zilker are kindly acknowledged for several fruitful discussions. Financial support from DFG within SFB 481 B2 and Z4 and financial support from BACATEC for a research visit at UCSB is gratefully acknowledged. Part of this work is based upon research conducted at the Cornell High-Energy Synchrotron Source (CHESS) which is supported by the National Science Foundation and the National Institutes of Health/National Institute of General Medical Sciences under Award DMR 9713424. T.B. also would like to thank the “Fonds der Chemischen Industrie” for a scholarship.

References and Notes

- (1) Hesselink, L.; Orlov, S. S.; Bashaw, M. C. *Proc. IEEE* **2004**, *92*, 1231.
- (2) Ashley, J.; Bernal, M. P.; Burr, G. W.; Coufal, H.; Guenther, H.; Hoffnagle, J. A.; Jefferson, C. M.; Marcus, B.; Macfarlane, R. M.; Shelby, R. M.; Sincerbos, G. T. *IBM J. Res. Dev.* **2000**, *44*, 341.
- (3) Waldman, D. A.; Butler, C. J.; Raguin, D. H. *Proc. SPIE* **2003**, *5216*, 10.

- (4) Barbastathis, G.; Psaltis, D. Volume holographic multiplexing methods. In *Holographic data storage*; Coufal, H., Psaltis, D., Sincerbox, G. T., Eds.; Springer-Verlag: Berlin, 2000.
- (5) Schnoes, M.; Ihas, B.; Dhar, L.; Michaels, D.; Setthachayanon, S.; Schomberger, G. L.; Wilson, W. L. *Proc. SPIE* **2003**, 4988, 68.
- (6) Eich, M.; Wendorff, J. H.; Ringsdorf, H.; Schmidt, H. W. *Makromol. Chem.* **1985**, 186, 2639.
- (7) Ringsdorf, H.; Schmidt, H. W.; Baur, G.; Kiefer, R.; Windscheid, F. *Liq. Cryst.* **1986**, 1, 319.
- (8) Eich, M.; Wendorff, J. H.; Peck, B.; Ringsdorf, H. *Makromol. Rapid Commun.* **1987**, 8, 59.
- (9) Meng, X.; Natansohn, A.; Rochon, P. *Polymer* **1997**, 38, 2677.
- (10) Cimrova, V.; Neher, D.; Kostromine, S.; Bieringer, T. *Macromolecules* **1999**, 32, 8496.
- (11) Hvilsted, S.; Andruzzi, F.; Kulinna, C.; Siesler, H. W.; Ramanujam, P. S. *Macromolecules* **1995**, 28, 2172.
- (12) Berg, R. H.; Hvilsted, S.; Ramanujam, P. S. *Nature (London)* **1996**, 383, 505.
- (13) Zilker, S. J.; Bieringer, T.; Haarer, D.; Stein, R. S.; Van Egmond, J. W.; Kostromine, S. G. *Adv. Mater.* **1998**, 10, 855.
- (14) Zilker, S. J.; Huber, M. R.; Bieringer, T.; Haarer, D. *Appl. Phys. B: Laser Opt.: Lasers Opt.* **1999**, 68, 893.
- (15) Hagen, R.; Bieringer, T. *Adv. Mater.* **2001**, 13, 1805.
- (16) Rochon, P.; Batalla, E.; Natansohn, A. *Appl. Phys. Lett.* **1995**, 66, 136.
- (17) Kim, D. Y.; Tripathy, S. K.; Li, L.; Kumar, J. *Appl. Phys. Lett.* **1995**, 66, 1166.
- (18) Natansohn, A.; Rochon, P. *Chem. Rev.* **2002**, 102, 4139.
- (19) Barrett, C. J.; Rochon, P. L.; Natansohn, A. L. *J. Chem. Phys.* **1998**, 109, 1505.
- (20) Lefin, P.; Fiorini, C.; Nunzi, J.-M. *Pure Appl. Opt.* **1998**, 7, 71.
- (21) Pedersen, T. G.; Johansen, P. M.; Holme, N. C. R.; Ramanujam, P. S.; Hvilsted, S. *Phys. Rev. Lett.* **1998**, 80, 89.
- (22) Viswanathan, N. K.; Balasubramanian, S.; Li, L.; Kumar, J.; Tripathy, S. K. *J. Phys. Chem. B* **1998**, 102, 6064.
- (23) Frenz, C.; Fuchs, A.; Schmidt, H.-W.; Theissen, U.; Haarer, D. *Macromol. Chem. Phys.* **2004**, 205, 1246.
- (24) Cui, L.; Tong, X.; Yan, X.; Liu, G.; Zhao, Y. *Macromolecules* **2004**, 37, 7097.
- (25) Mao, G.; Wang, J.; Clingman, S. R.; Ober, C. K.; Chen, J. T.; Thomas, E. L. *Macromolecules* **1997**, 30, 2556.
- (26) Moriya, K.; Seki, T.; Nakagawa, M.; Mao, G.; Ober, C. K. *Macromol. Rapid Commun.* **2000**, 21, 1309.
- (27) Tian, Y.; Watanabe, K.; Kong, X.; Abe, J.; Iyoda, T. *Macromolecules* **2002**, 35, 3739.
- (28) Hayakawa, T.; Horiuchi, S.; Shimizu, H.; Kawazoe, T.; Ohtsu, M. *J. Polym. Sci., Part A: Polym. Chem.* **2002**, 40, 2406.
- (29) Tong, X.; Cui, L.; Zhao, Y. *Macromolecules* **2004**, 37, 3101.
- (30) Wang, G.; Tong, X.; Zhao, Y. *Macromolecules* **2004**, 37, 8911.
- (31) Han, Y.-K.; Dufour, B.; Wu, W.; Kowalewski, T.; Matyjaszewski, K. *Macromolecules* **2004**, 37, 9355.
- (32) Yoshida, E.; Ohta, M. *Colloid Polym. Sci.* **2005**, 283, 521.
- (33) Ravi, P.; Sin, S. L.; Gan, L. H.; Gan, Y. Y.; Tam, K. C.; Xia, X. L.; Hu, X. *Polymer* **2005**, 46, 137.
- (34) Cui, L.; Zhao, Y.; Yavrian, A.; Galstian, T. *Macromolecules* **2003**, 36, 8246.
- (35) Schneider, A.; Zanna, J.-J.; Yamada, M.; Finkelmann, H.; Thomann, R. *Macromolecules* **2000**, 33, 649.
- (36) Zhao, Y.; Bai, S.; Asatryan, K.; Galstian, T. *Adv. Funct. Mater.* **2003**, 13, 781.
- (37) Osuji, C. O.; Chen, J. T.; Mao, G.; Ober, C. K.; Thomas, E. L. *Polymer* **2000**, 41, 8897.
- (38) Yu, H.; Okano, K.; Shishido, A.; Ikeda, T.; Kamata, K.; Komura, M.; Iyoda, T. *Adv. Mater.* **2005**, 17, 2184.
- (39) Morikawa, Y.; Nagano, S.; Watanabe, K.; Kamata, K.; Iyoda, T.; Seki, T. *Adv. Mater.* **2006**, 18, 883.
- (40) Haeckel, M.; Kador, L.; Kropp, D.; Frenz, C.; Schmidt, H.-W. *Adv. Funct. Mater.* **2005**, 15, 1722.
- (41) Haeckel, M.; Kador, L.; Frenz, C.; Schmidt, H.-W. *Proc. SPIE* **2004**, 5521, 63.
- (42) Minabe, J.; Maruyama, T.; Yasuda, S.; Kawano, K.; Hayashi, K.; Ogasawara, Y. *Jap. J. Appl. Phys.* **2004**, 43, 4964.
- (43) Haeckel, M.; Kador, L.; Kropp, D.; Frenz, C.; Schmidt, H.-W. *Proc. SPIE* **2005**, 5939, 593908/1.
- (44) Haeckel, M.; Kador, L.; Kropp, D.; Schmidt, H.-W. *Adv. Mater.* **2007**, 19, 227.
- (45) Allen, R. D.; Long, T. E.; McGrath, J. E. *Polym. Bull.* **1986**, 15, 127.
- (46) Hirao, A.; Kato, H.; Yamaguchi, K.; Nakahama, S. *Macromolecules* **1986**, 19, 1294.
- (47) Mori, H.; Wakisaka, O.; Hirao, A.; Nakahama, S. *Macromol. Chem. Phys.* **1994**, 195, 3213.
- (48) Breiner, T.; Schmidt, H.-W.; Muller, A. H. E. *e-Polym.* **2002**, Paper No 22.
- (49) Theissen, U.; Zilker, S. J.; Pfeuffer, T.; Strohriegel, P. *Adv. Mater.* **2000**, 12, 1698.
- (50) Kogelnik, H. *Bell Syst. Tech. J.* **1969**, 48, 2909.
- (51) Bohnert, R.; Finkelmann, H. *Macromol. Chem. Phys.* **1994**, 195, 689.
- (52) Yamada, M.; Hirao, A.; Nakahama, S.; Iguchi, T.; Watanabe, J. *Macromolecules* **1995**, 28, 50.
- (53) Adams, J.; Gronski, W. *Makromol. Rapid Commun.* **1989**, 10, 553.
- (54) Saenger, J.; Gronski, W. *Macromol. Chem. Phys.* **1998**, 199, 555.
- (55) Jeuck, H.; Mueller, A. H. E. *Makromol. Rapid Commun.* **1982**, 3, 121.
- (56) Tuzar, Z.; Kratochvil, R.; Chapter 1. In *Surface and Colloid Science*; Matijevic, E., Ed.; Plenum Press: New York, 1993; Vol. 15, p 1.
- (57) Pan, J.; Chen, M.; Warner, W.; He, M.; Dalton, L.; Hogen-Esch, T. E. *Macromolecules* **2000**, 33, 7835.
- (58) Breiner, U.; Krappe, U.; Thomas, E. L.; Stadler, R. *Macromolecules* **1998**, 31, 135.
- (59) Abetz, V.; Goldacker, T. *Macromol. Rapid Commun.* **2000**, 21, 16.
- (60) Alexander, P.; Charlesby, A. *Nature (London)* **1954**, 173, 578.
- (61) Yokoyama, H.; Mates, T. E.; Kramer, E. J. *Macromolecules* **2000**, 33, 1888.
- (62) Bates, F. S.; Berney, C. V.; Cohen, R. E. *Macromolecules* **1983**, 16, 1101.
- (63) Hashimoto, H.; Fujimura, M.; Hashimoto, T.; Kawai, H. *Macromolecules* **1981**, 14, 844.
- (64) Mayes, A. M.; Russell, T. P.; Satija, S. K.; Majkrzak, C. F. *Macromolecules* **1992**, 25, 6523.
- (65) Ueda, M.; Kim, H.-B.; Ikeda, T.; Ichimura, K. *J. Non-Cryst. Solids* **1993**, 163, 125.
- (66) Mita, I.; Horie, K.; Hirao, K. *Macromolecules* **1989**, 22, 558.
- (67) Brown, D.; Natansohn, A.; Rochon, P. *Macromolecules* **1995**, 28, 6116.
- (68) Natansohn, A.; Rochon, P.; Ho, M.-S.; Barrett, C. *Macromolecules* **1995**, 28, 4179.
- (69) Rau, H.; In *Photochemistry and Photophysics*; Rabek, J. K., Ed.; CRC Press: Boca Raton, FL, 1990; Vol. 2, p 119.

MA0624907